

# Strength and stiffness properties of stonewool used as cloudburst reservoir under roads

Niels Trads<sup>1</sup>, Nataša Katić<sup>1</sup>

<sup>1</sup>Geo, Maglebjergvej 1, 2800 Kongens Lyngby, Denmark

nit@geo.dk

**Abstract.** With the climate change, Copenhagen has seen an increase in cloudbursts. During the cloudbursts, sewer systems overflow and result in flooded basements and overspill of untreated water into the harbour. A solution to the limited capacity is to make cloudbursts reservoirs to delay the rain water filling the sewer system. At Langelands Plads in Copenhagen, a reservoir has been established using the stonewool product Rockflow. The Rockflow is installed under two roads and a space used for recreational purposes. Based on monotonic and cyclic laboratory tests, material parameters and appropriate numerical model for the anisotropic material were established. In-situ measurements of the stiffness during and after installation at Langelands Plads consisted of plate load tests and falling weight deflectometer tests together with rutting measurements. The in-situ measurements were statistically processed and back-analysed to confirm the initial material parameters and model. Further, the in-situ measurements are ongoing at appropriate intervals to monitor the performance of the road.

## 1. Introduction

At Langelands Plads in Copenhagen Rockflow is used as a cloudburst reservoir for delayed filling of the sewer system. The Rockflow is installed in a 0.5 m thick layer under two roads and a space used for recreational purposes. The road construction on top of the elements consists of 0.4 m of compacted gravel and 0.12 m of asphalt.

Rockflow is a high porosity material of mineral origin. The structure of the material in general, and elements made out of it, is visibly fibrous. Due to the structure of the material, the mechanical behavior of the material is orthotropic.

The available information consists of laboratory tests and in-situ tests. The laboratory tests comprised unconfined compressive strength tests and monotonic and cyclic triaxial tests. The in situ tests consisted of plate load tests and falling weight deflectometer tests.

The project task was to evaluate mechanical properties of the Rockflow material and to derive a consistent set of material parameters for Rockflow based on laboratory and in situ tests. Upon reviewing the available information from laboratory and in situ tests, the results are back-analysed and essential numerical modelling is conducted using Plaxis 2D software. The appropriate numerical model to capture the anisotropic behaviour of elements stacked next to each other was chosen; where no parameters were available, a parametric study was conducted to evaluate influence of the chosen parameters.

## 2. Rockflow material and design of pavement on top

The used Rockflow material was commercially available in several types with different densities [1]. The structure of the material in general, and elements made out of it, is visibly fibrous. The type primarily used for Langelands Plads was WM2007, with the general material parameters summarized in Table 1.

**Table 1.** General material parameters for Rockflow WM2007.

Material type	[-]	WM2007
Element dimensions [y*x*z]	[m]	1.0 x 1.2 x 0.75
Mass per element	[kg]	15
Porosity	[%]	94
Dry density	[g/cm <sup>3</sup> ]	0.166
Void ratio	[-]	15.7
Bulk density, fully saturated	[g/cm <sup>3</sup> ]	1.11
Unit Weight, effective	[kN/m <sup>3</sup> ]	1.63
Unit Weight, total	[kN/m <sup>3</sup> ]	10.8
Grain density	[g/cm <sup>3</sup> ]	2.77

A Rockflow element is shown in Figure 1. The elements are anisotropic and the definition of x, y and z directions is shown in Figure 2. The elements for the road at Langelands Plads were placed with the y-direction corresponding to vertical direction and the x-direction being parallel to the road.



**Figure 1.** Rockflow element.

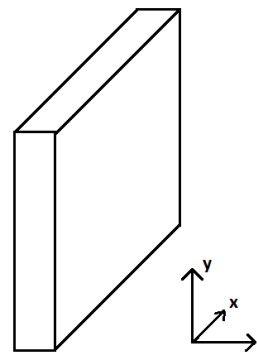


**Figure 2.** Definition of directions for the Rockflow element.

The design of the pavement used at Langelands Plads is shown in Table 2. The Rockflow was placed on top the subsoil. The pavement on top of the Rockflow, consisted of 400 mm of compacted gravel followed by 120 mm of asphalt.

**Table 2.** General cross section at Langelands Plads.

Layer no.	Description	Thickness
[-]	[-]	[mm]
1	Asphalt, AB 160/220	25
2	Asphalt, GAB I 70/100	95
3	Compacted gravel, SG II	400
4	Rockflow, WM 2007	500
5	Subsoil	-

### 3. Laboratory tests

Laboratory tests for determination of strength and stiffness parameters were planned and conducted at Deltares laboratory [2] and consisted of unconfined compressive strength (UCS) tests, monotonic triaxial tests and cyclic triaxial tests. Specimens for testing were prepared from the elements.

The UCS tests were conducted on specimens prepared with different orientation and with different degree of saturation. The stress-strain curves from the UCS tests presented in Figure 3 show that the strength and stiffness depends on the direction and degree of saturation. The material has the highest strength and stiffness in the y direction. The failure in the z-direction is ductile, occurring above 20% strain, whereas in the y- and x-directions, the material fails at a more brittle failure at strain levels of 2.4% – 3.3%. The ratios of the strength and stiffness in the x- and z-direction, to the strength and stiffness in the y-direction are presented in Table 3. Reduction of strength as the saturation is increased from 10 to 100% is the highest in z-direction (28%), and the smallest in y-direction (5%).

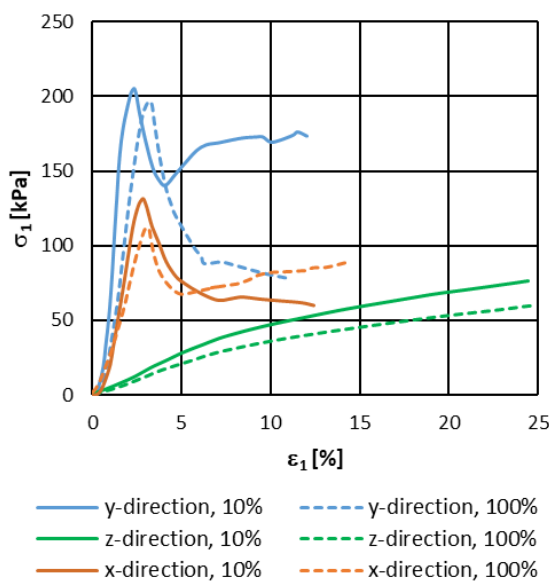


**Figure 3.** Stress-strain relation for UCS tests with different specimen orientation and degree of saturation.

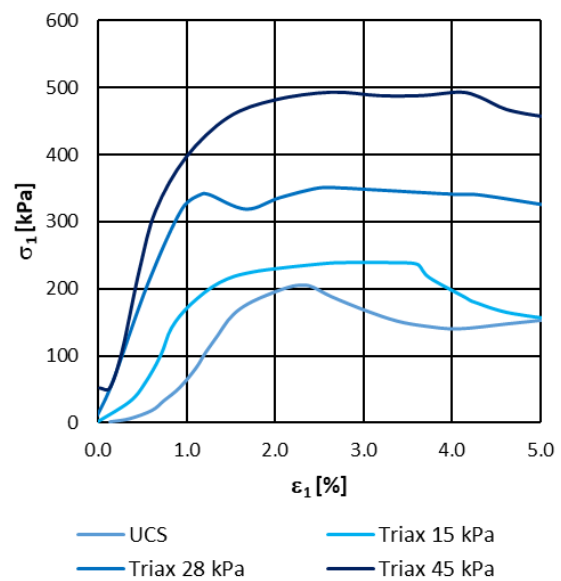


**Figure 4.** Stress-strain relation for UCS and monotonic triaxial tests for specimens tested in y-direction with 10% saturation.

**Table 3.** Ratios between strength in different directions, stiffness in different directions and degree of saturation.

	y-direction	x-direction	z-direction
Unconfined compressive strength, $\sigma_c$ , 10% saturation	1.00	0.64	0.38
Unconfined compressive strength, $\sigma_c$ , 100% saturation	0.96	0.54	0.29
Young's modulus, $E_{50}$ , 10% saturation	1.00	0.46	0.06
Young's modulus, $E_{50}$ , 100% saturation	0.66	0.38	0.05

The monotonic and cyclic triaxial tests were conducted on specimens prepared in the y-direction, corresponding to vertical direction when the elements are used in the pavement. The monotonic triaxial tests were conducted with 10 % saturation and cell pressures ranging from 15 kPa to 45 kPa and were conducted to determine the drained strength parameters and the effect of confining pressure on the stiffness. The stress-strain curves from the tests are shown in Figure 4. The peak strength is shown in Figure 5 where the interpreted friction angle and cohesion are given. The variation of Young's modulus,  $E_{50}$ , as a function of confining pressure is given in Figure 6, where it is seen that Young's modulus varies linearly with the confining pressure.

The cyclic triaxial test was conducted to determine the influence of cyclic loading on the stiffness. The test was conducted with 5 kPa confining pressure and 100000 cycles with an amplitude of  $\sigma_1 = 85$  kPa. The resilient Young's modulus ( $E_{resilient} = 33$  MPa) determined during the cyclic loading was significantly higher than the Young's modulus determined during the virgin loading in the monotonic tests. Further, after 100000 cycles and  $\sim 2.5\%$  axial strain the specimen was loaded to monotonic failure and the strength was found to be slightly above the strength determined from the monotonic tests. See Figure 5. For the application of traffic load, the resilient modulus is considered most relevant.

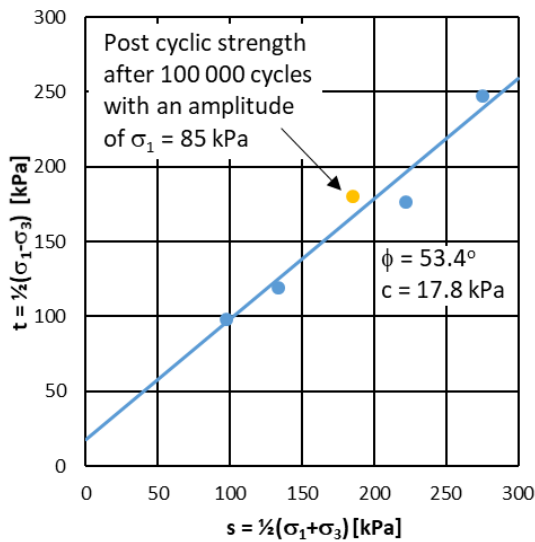


**Figure 5.** Determination of drained strength parameters.

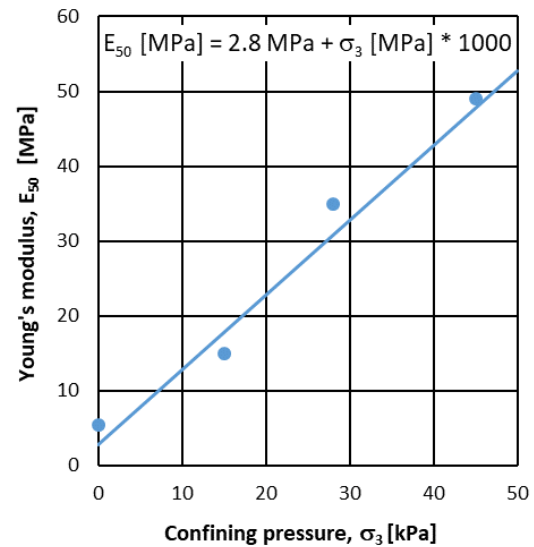


**Figure 6.** Effect of confining pressure on stiffness.

The parameters in the x- and z-directions are obtained using the ratios of UCS strength and stiffness from Table 3. Using the Mohr-Coulomb failure criterion and the boundary conditions of the UCS test, the drained strength parameters in the x- and z-directions are determined as:

$$\frac{c_y + \sigma \tan \phi_y}{c_i + \sigma \tan \phi_i} = \frac{q_{uy}}{q_{ui}}; \text{ with } \frac{c_y}{c_i} = \frac{q_{uy}}{q_{ui}} \text{ in UCS test, for } i = \{x; z\}$$

All parameters derived from the laboratory tests and used for further analysis are summarized in Table 4. As a fundamental assumption, Poisson's ratio of 0 has been used for the simulations. This value has been assumed by Lapinus based on their experience with the material. Considering the structure of the material and very low elastic capacity of the material, technical difficulties of measurements for evaluation of Poisson's ratio are significant. It was hence, decided to parametrically study the effect of the variation of the Poisson's ratio.

**Table 4.** Summary of strength and stiffness parameters determined from laboratory tests.

Parameter	Unit	y-direction	x-direction	z-direction
Friction angle	[°]	53.4	37.6	22.4
Cohesion	[kPa]	17.8	11.4	6.7
Young's modulus, $E_{50}$	[MPa]	$3.8 + \sigma_3 * 1000$	$1.7 + \sigma_3 * 455$	$0.2 + \sigma_3 * 63$
Resilient Young's modulus, $E_{resilient}$	[MPa]	33	-	-
Poisson's ratio, $\nu$	[-]	0.00	0.00	0.00

#### 4. In-situ tests

The in-situ tests consisted of plate load tests and falling weight deflectometer (FWD). The plate load tests were conducted on top of different layers during the construction. This is shown in Table 5. The FWD tests were conducted on the finished road.

The results from the plate load tests are shown in Figure 7. The plate load tests were conducted with unloading-reloading cycles during the tests. It was not possible to conduct the plate load tests directly on top of the Rockflow. The large difference in results between the two plate load tests on gravel is believed to be due to a local variation in gravel compaction at the “Gravel II” measurement.

**Table 5.** Overview of in-situ tests on Rockflow at Langelands Plads.

Layer no. [-]	Description [-]	Thickness [mm]	Number of plate load tests	Number of FWD
1	Asphalt, AB 160/220	25	2	11
2	Asphalt, GAB I 70/100	95	-	-
3	Compacted gravel, SG II	400	2	-
4	Rockflow, WM 2007	500	-	-
5	Subsoil	-	1	-

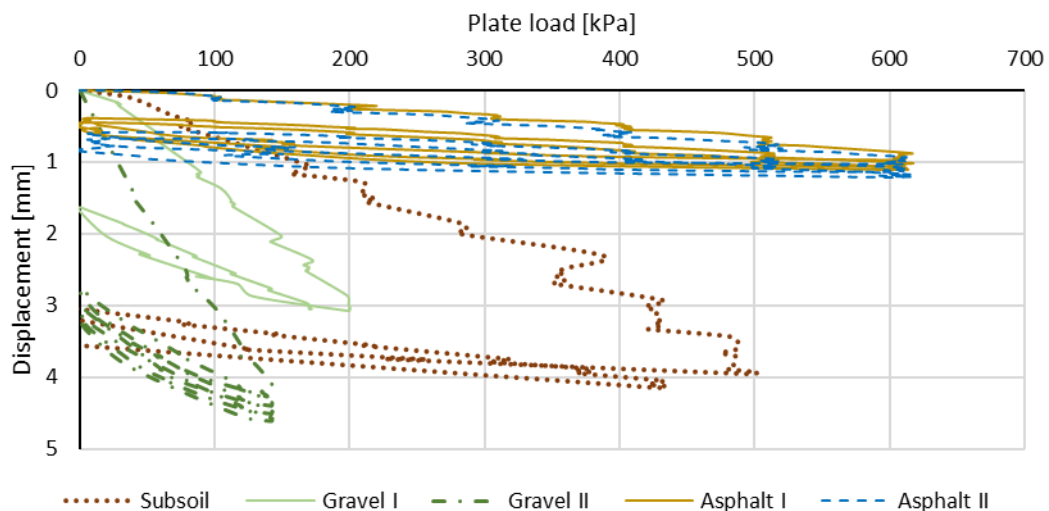


**Figure 7.** Stress-strain relation for UCS tests with different specimen orientation and degree of saturation.

The results of the FWD tests are given in Table 6, as the stiffness of the asphalt layers, compacted gravel and Rockflow elements, respectively. It was not possible to distinguish the stiffness of the two asphalt layers from each other and it was not possible to distinguish the stiffness of the Rockflow from the stiffness of the subsoil in the interpretation of the FWD tests. The results in Table 6 are determined as a mean value and with 95% confidence intervals using bootstrap resampling methodology. Resilient modulus of the Rockflow cf. Table 4 of 33 MPa fits well within the 95% confidence interval of  $E_{FWD, mean}$  values (28-63 MPa) evaluated for the Rockflow based on falling weight tests.

**Table 6.** Summary of stiffness determined from FWD tests.

	Unit	Asphalt AB/GAB	Gravel	Rockflow
$E_{FWD, mean}$	[MPa]	4960	240	45
$E_{FWD, 95\% \text{ confidence interval, low}}$	[MPa]	3840	150	28
$E_{FWD, 95\% \text{ confidence interval, high}}$	[MPa]	6220	370	63

## 5. Back analysis and comparison between parameters determined in laboratory and in-situ

Numerical modelling is performed using Plaxis 2D Version 2018.01 and the SoilTest option within Plaxis [3]. The essential material parameters were fitted using the linear elastic - Mohr-Coulomb plastic material model (MC) to back-analyse the laboratory tests using SoilTest option. Thereafter, MC and the Jointed Rock model (JR) were used for back analysis of the field tests.

The Jointed Rock model is an anisotropic elastic perfectly-plastic model. In this model it is assumed that there is intact material with an optional stratification direction, herein x-z plane, and major joint direction, herein interpreted as the y-direction. The intact material is considered to behave as a transversely anisotropic elastic material, quantified by five parameters and a direction. The anisotropy may result from stratification or from other phenomena. Here it is used to model the Rockflow elements as used in the pavement. In the major joint direction (here: y) it is assumed that shear stresses are limited according to Mohr-Coulomb's criterion. Upon reaching the maximum shear stress in the joint direction, plastic sliding will occur. In general, a maximum of three sliding directions ('planes') can be defined, of which the first plane is assumed to coincide with the direction of elastic anisotropy. Each plane may have different shear strength properties. In addition to plastic shearing, the tensile stresses perpendicular to the three planes are limited according to a predefined tensile strength (tension cut-off).

The application of the Jointed Rock model is justified when families of joints or joint sets are present. These joint sets have to be parallel, not filled with fault gouge, and their spacing has to be small compared to the characteristic dimension of the structure. Herein, this is interpreted as the dominant Rockflow fiber direction, considering that the fibers and their spacing are of much smaller dimension than the elements. A reservation towards the model is made that the fibers of the Rockflow are realistically neither ideally parallel nor straight, but some alignment is visible. The additional parameters required for the Jointed Rock model are described in Table 7.

**Table 7.** Additional parameters for the Joint Rock model.

Parameter	Unit		Notes
$\alpha_{1,y}$	[°]	90	Defines the joints in vertical direction
$\alpha_{1,z}$	[°]	0	Defines the joints in horizontal direction
Shear modulus, $G_z$	[kPa]	450	Defines the joint stiffness. Given as: $G = E/2$ for $\nu = 0$

### 5.1. Back-analysis of laboratory tests

Simulation using the linear elastic - Mohr-Coulomb plastic material (MC) using Plaxis SoilTest for the three monotonic triaxial tests in y-direction are presented on Figure 8. Using the variation of Young's modulus with confining pressure as defined in Table 3, the behaviour observed in the laboratory tests are captured in the back-analysis.

Joint rock material model cannot be modelled using SoilTest module of Plaxis. For the evaluation of the JR and comparison with the MC, a 2D model of a footing on Rockflow is made using Plaxis. The model assumes no loading history of the Rockflow material, hence the assumed elastic parameters correspond to a confinement levels of approximately 15 kPa.

For a comparison, the same situation is modelled using MC and JR models, and the output of the same material point using the two material models is presented on Figure 9 and compared with the corresponding triaxial test. The Young's modulus  $E_{50}$  is applicable for the first loading cases, whereas in the repeated loading and/or upon repeated loading, resilient or post-cyclic Young's modulus  $E_{resilient}$  are considered appropriate. Plaxis simulation shows that the results obtained using MC and JR models are similar, which is largely due to the fact that the models are using the same parameters for the loading direction. The slight overshooting of the strength seen in the results using the JR model is a consequence of the modulus  $G_z$ , affecting the failure mode.

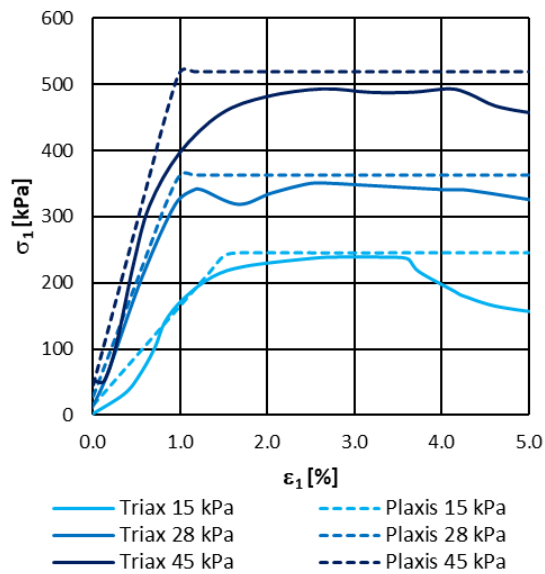


**Figure 8.** Comparison of measured stress strain and Plaxis SoilTest simulation results using linear elastic, Mohr Coulomb plastic parameters.

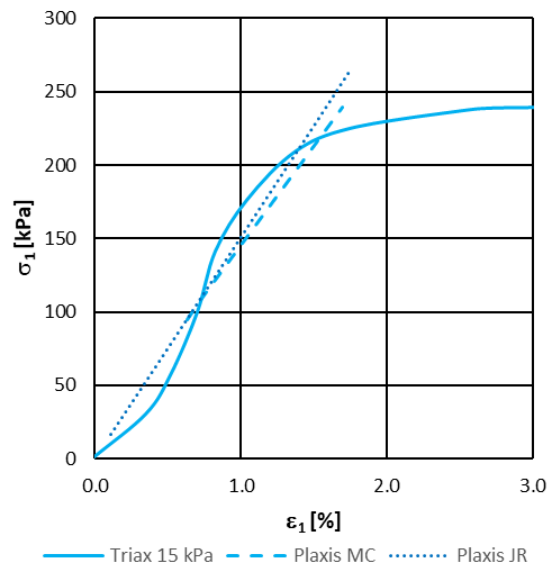


**Figure 9.** Comparison of elastic response from triaxial tests with (MC) and (JR) from Plaxis.

Based on the observed results, for the analyses of loads in y-direction, anisotropy has little influence and can be neglected. More so, it is found sufficient and appropriate to use 2D models.

The development of failure using JR model favours the prescribed joint directions. In Figure 10, the failure figure obtained using the MC model is compared with the results of the JR model. The JR model is shown with and without joint strength, corresponding to reduction of the  $G_z$  modulus. In case of diminishing modulus, the failure predicted by JR model is pure penetration along the defined joint direction (y). Increase of the modulus  $G_z$  brings the predicted failure to the similar zones as predicted by MC model, without a significant influence on the compressional response in terms of vertical deformation of the surface.

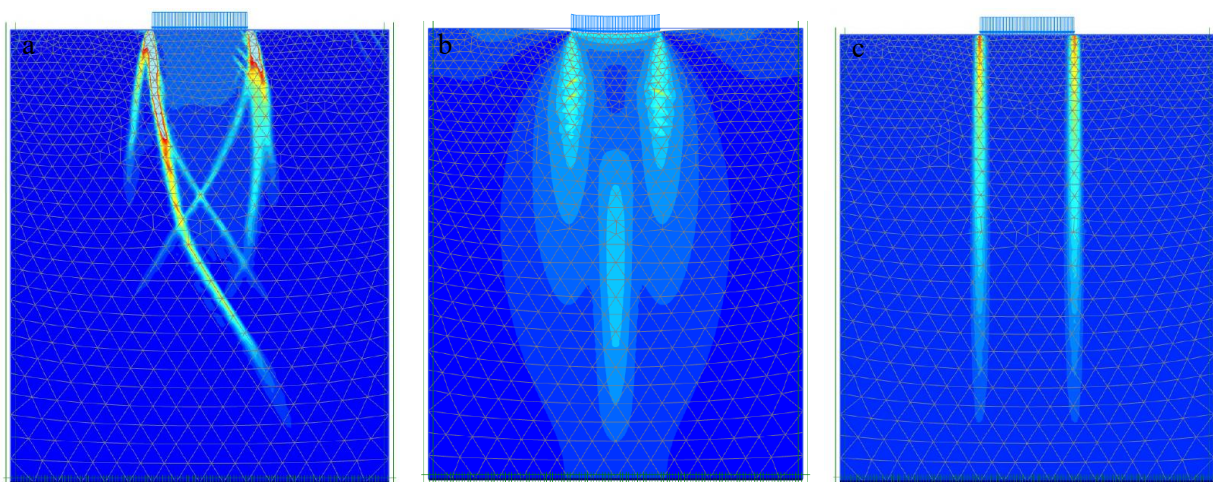


**Figure 10.** Failure figure of shallow footing placed directly on Rockflow elements using a) Mohr Coulomb model b) Joint rock model with strength between the elements c) Joint rock model without strength between the elements.

Numerical studies have shown that the effect of the Poisson's ratio is negligible. The Plaxis simulations have shown that the near surface failure figure below a loaded plate is nearly vertical regardless of the choice of the model in case of the Poisson's ratio of 0. In case of Poisson's ratio higher than 0 governing the interaction between the joints in JR model, the failure figure approaches the MC failure figure in terms of depth and the most loaded zones. As no physical tests on this type of material have been carried out to the limit of fully developed failure, no failure figure is deemed more realistic than the other.

5.2. Back-analysis of in situ tests

The back-analysis of the plate load tests was conducted with the main goal to confirm the applicability of the resilient modulus from the laboratory testing on Rockflow for design purposes. In addition to this, the analysis was conducted to reveal the effect of variations of the material parameters for compacted gravel on overall assessment of the Rockflow modulus. All the materials other than the Rockflow were modelled as linear elastic. The material parameters used for the individual layers are summarized in Table 8.

**Table 8.** Summary of material parameters for the back-analysis of plate load tests.

Parameter	Unit	Subsoil	Rockflow	Gravel	Asphalt
Unit Weight, effective	[kN/m <sup>3</sup> ]	21	11.1	21	24
Unit Weight, total	[kN/m <sup>3</sup> ]	21	1.83	20	24
Friction angle	[°]	-	53.4	-	-
Cohesion	[kPa]	-	17.8	-	-
Resilient Young's modulus, E <sub>resilient</sub>	[MPa]	87	45	240	4960
Poisson's ratio, ν	[-]	0.30	0	0.35	0.35
Interface stiffness, R <sub>inter</sub>	[-]	1.00	0.67	1.00	1.00

The back-analysis was conducted with loading corresponding to the plate load tests. The results of the back-analysis are compared with the plate load tests in Figure 11, where Phase 1 represents loading directly on the subsoil, Phase 2 on the compacted gravel and Phase 4 on the asphalt AB layer. An overall good agreement is found.

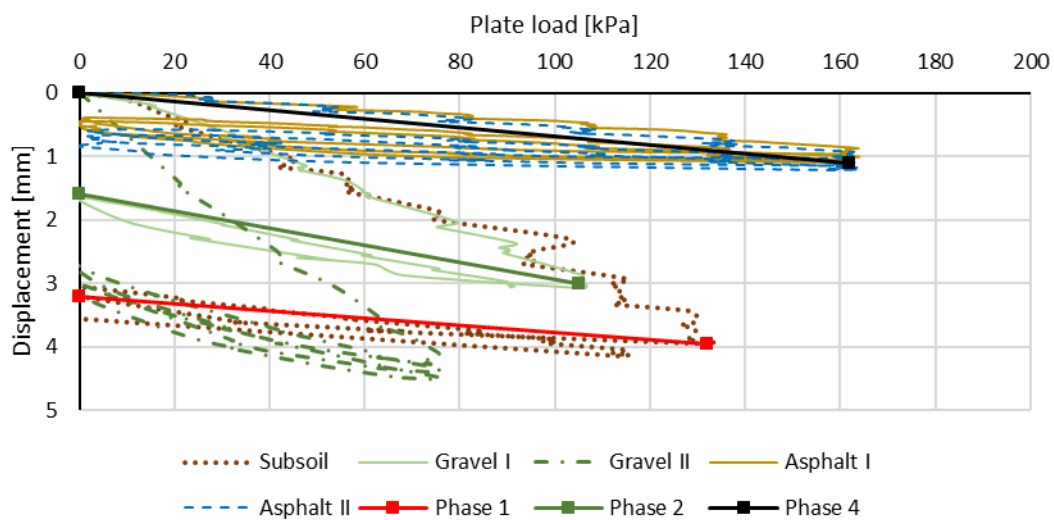


**Figure 11.** Comparison of results and back-analysis of plate load tests.

The vertical stresses and vertical strains for the MC and JR models are shown in Figure 12 and Figure 13, respectively. The stress concentrations directly underneath the edges of the plates during the plate load tests are a consequence of the load modelled as uniformly distributed across the equivalent plate, rather than uniformly distributed across the original, round, plate. The effect of these concentrations vanishes in the topmost compacted gravel and is considered negligible, i.e. below this zone, the load on the soil/Rockflow is sufficiently uniform.

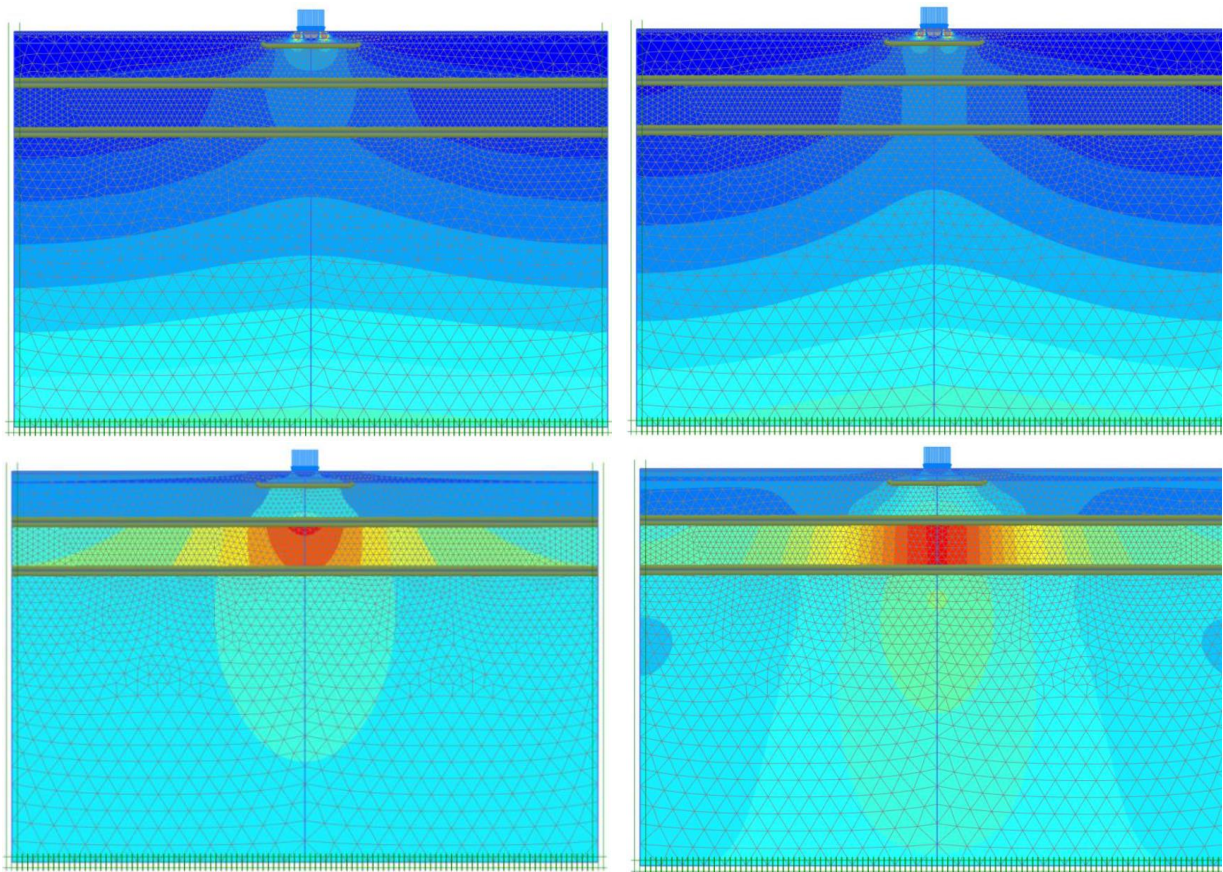


**Figure 12.** Top, vertical effective stresses under plate load on top of asphalt layer, using MC model. Bottom, vertical strain under plate load on top of asphalt layer, using MC model.

**Figure 13.** Top, vertical effective stresses under plate load on top of asphalt layer, using JR model. Bottom, vertical strain under plate load on top of asphalt layer, using JR model.

The pressure on the surface of compacted gravel did not exceed 300 kPa in tests carried out directly on the compacted gravel surface nor in the tests carried out on asphalt concrete surface due to the load spreading through asphalt concrete layers. This pressure is well below the bearing capacity of gravels. Therefore, it is considered appropriate to apply linear elastic model.

Back-analysis of tests on compacted gravel and asphalt layers show a relatively good match with the measured values. However, the results on asphalt does show less stiff response than the measured ones. Considering a high variation of the elastic moduli of asphalt concrete based on FWD tests the result is interpreted as a likely consequence of the variation of the moduli across the site.

By conducting a parametric study of the elastic parameters, the following was observed:

- As expected, decreasing the stiffness lead to increase of settlements, and vice versa
- The minimum parameters match the reloading branch of the Gravel I rather accurately.
- Majority of the vertical deformation comes from the Rockflow cluster, indicating that the overlying layers are sufficiently compacted.

- The horizontal tension in the Rockflow elements is concentrated in the zone directly under the plate and is calculated as max 1.5 N. This is considered negligible.
- The influence of weaker interface between the Rockflow elements and compacted gravel and/or intact soil is diminutive and can be neglected.

The application of the Joint rock model (JR) leads to somewhat higher vertical deformations than the linear elastic – Mohr Coulomb plastic material model. The results show that the application of the JR model in combination with the mean material parameters results in the very good match for the plate load tests on compacted gravel. This indicates that it is appropriate to apply the same scaling for the resilient modulus between y- and z-directions as applied to  $E_{50}$ . Finally, the analyses using the JR model are equivalent to the analysis using the lower bound parameters, indicating that the lower bound parameters are appropriate as characteristic values for further design purposes.

## 6. Conclusion

A consistent set of material parameters for Rockflow based on laboratory and in situ tests has been derived. The tests were back-analysed and the parameters confirmed using the linear elastic Mohr-Coulomb plastic model in Plaxis. Further, using the Joint Rock model, it was possible to model the reduced friction between the elements of Rockflow used in the reservoir at Langelands Plads.

## Acknowledgement

The authors would like to express gratitude to Lapinus and the Frederiksberg Municipality for the permission to publish data. Findings and conclusions expressed in this paper do not necessarily reflect the views of Lapinus.

## References

- [1] Lapinus. Product data sheet Rockflow elements. Stone wool elements for water management. Revision date December 2017
- [2] Deltares. Lapinus mineral wool test analysis and interpretation, Suggested applications under trafficked areas, Deltares reference: 11200122-000-GEO-0007-gbh, 2018
- [3] Plaxis 2D 2019 Material Models Manual. <https://www.plaxis.com/support/manuals/plaxis-2d-manuals/>
- [4] Geo. Brug af produktet Rockflow i vejopbygning, Pladebelastningsforsøg, minifaldlodsmålinger, faldlodsmålinger, måling af tværsnitsprofiler samt trafikmålinger, Frederiksberg. Langelands Plads, Geo projekt nr. 202895, Rapport 4,
- [5] Geo. Rockflow. Material Interpretation Report, Back Analysis of laboratory tests carried out by Deltares (ATR 01-01) Geo projekt nr. 202895, Rapport 5, 2019-02-26
- [6] Geo. Rockflow. Material Interpretation Report, Back Analysis of plate load tests carried out at Langelands Plads (ATR 01-02), Geo projekt nr. 202895, Rapport 6, 2019-07-17